Addiction Biology

SSA SOCIETY FOR THE STUDY OF ADDICTION

HUMAN NEUROIMAGING STUDY

doi:10.1111/adb.12285

Disrupted white matter structural connectivity in heroin abusers

Yan Sun[1,7*], Gui-Bin Wang[2*], Qi-Xiang Lin[3*], Lin Lu[1,4,5,7], Ni Shu[3], Shi-Qiu Meng[1,4,5,7], Jun Wang[3], Hong-Bin Han[6], Yong He[3] & Jie Shi[1,7,8,9]

National Institute on Drug Dependence, Peking University, China[1], Institute of Materia Medical, Chinese Academy of Medical Sciences and Peking Union Medical College, China[2], State Key Laboratory of Cognitive Neuroscience and Learning and IDG/McGovern Institute for Brain Research, Beijing Normal University, China[3], Peking-Tsinghua Center for Life Sciences and PKU-IDG/McGovern Institute for Brain Research, Peking University, China[4], Key Laboratory of Mental Health, Institute of Mental Health, Peking University Sixth Hospital, China[5], Radiology Department, Peking University Third Hospital, China[6], Beijing Key Laboratory on Drug Dependence Research, China[7], The State Key Laboratory of Natural and Biomimetic Drugs[8] and Key Laboratory for Neuroscience of the Ministry of Education and Ministry of Public Healthy, Beijing, China[9]

ABSTRACT

Neurocognitive impairment is one of the factors that put heroin abusers at greater risk for relapse, and deficits in related functional brain connections have been found. However, the alterations in structural brain connections that may underlie these functional and neurocognitive impairments remain largely unknown. In the present study, we investigated topological organization alterations in the structural network of white matter in heroin abusers and examined the relationships between the network changes and clinical measures. We acquired diffusion tensor imaging datasets from 76 heroin abusers and 78 healthy controls. Network-based statistic was applied to identify alterations in interregional white matter connectivity, and graph theory methods were used to analyze the properties of global networks. The participants also completed a battery of neurocognitive measures. One increased subnetwork characterizing widespread abnormalities in structural connectivity was present in heroin users, which mainly composed of default-mode, attentional and visual systems. The connection strength was positively correlated with increases in fractional anisotropy in heroin abusers. Intriguingly, the changes in within-frontal and within-temporal connections in heroin abusers were significantly correlated with daily heroin dosage and impulsivity scores, respectively. These findings suggest that heroin abusers have extensive abnormal white matter connectivity, which may mediate the relationship between heroin dependence and clinical measures. The increase in white matter connectivity may be attributable to the inefficient microstructure integrity of white matter. The present findings extend our understanding of cerebral structural disruptions that underlie neurocognitive and functional deficits in heroin addiction and provide circuit-level markers for this chronic disorder.

Keywords Diffusion tensor imaging, heroin abuse, neurocognition, white matter, white matter connectivity.

Correspondence to: Jie Shi, National Institute on Drug Dependence, Peking University, 38 Xue Yuan Road, Beijing 100191, China.
E-mail: shijie@bjmu.edu.cn
Yong He, State Key Laboratory of Cognitive Neuroscience and Learning, Beijing Normal University, Beijing 100875, China. E-mail: yong.he@bnu.edu.cn

INTRODUCTION

Dependence on heroin results in high rates of mortality, morbidity and criminality and has become an important public health concern (Hulse *et al.* 1999). Extensively disrupted components in whole brain structures have been identified in heroin-addicted patients. Gray matter atrophy in heroin abusers mainly occurs in frontal and cingulate cortices (Liu *et al.* 2009). Several diffusion tensor imaging (DTI) studies have reported abnormal white matter integrity, including fractional anisotropy (FA), mean diffusivity, axial diffusivity and radial diffusivity, in specific brain structures, such as the corpus callosum and frontal matter, in heroin-dependent individuals (Liu *et al.*, 2008; Shen *et al.* 2012), but the results have been inconsistent (Bora *et al.* 2012; Qiu *et al.* 2013). Although

*These authors equally contributed to this work.

these previous imaging studies provided valuable information on the neuro-anatomical basis of addiction from segregated brain areas, a whole-system-level understanding is still lacking. The abnormal organization of function connectivity has also been revealed in heroin abusers by both task-related functional magnetic resonance imaging (fMRI; Wang *et al.* 2010) and resting-state fMRI (Yuan *et al.* 2010). However, still unclear is the structural basis of these functional network changes in heroin addiction. The present study investigated alterations in the topological organization of the structural network of white matter in heroin abusers.

Connectomics, which conceptualizes the whole brain as an interconnected network, is a promising approach for identifying circuit-level makers of this chronic disorder (Behrens & Sporns 2012). DTI is a primary method for characterizing the brain's white matter microstructure or 'structural network' *in vivo* (Hagmann *et al.* 2008). Graph theory enables analyses of the whole brain efficiency of information processing and specific network properties (Bullmore & Sporns 2009). Network-based statistic (NBS) can be used to identify differences in specific connections within a network between groups. Recent advances in NBS analysis have allowed better representations of the overall connectivity architecture, termed the human connectome. This allows us to understand psychiatric disorders based on brain connection abnormalities (Zalesky, Fornito, & Bullmore 2010). The structural connectivity of white matter can be well identified by the combined use of these approaches.

The default mode network (DMN) is a constellation of brain regions that represent a 'sentinel' resting state and internally oriented cognition (Buckner, Andrews-Hanna, & Schacter 2008). Many neuropsychiatric disorders are associated with abnormal function of the DMN (Whitfield-Gabrieli & Ford 2012). Resting-state functional connectivity alterations in the DMN have been found in heroin abusers (Hu *et al.* 2012). Brain regions that are involved in the DMN, such as the anterior cingulate cortex and hippocampus, play an important role in heroin addiction-related cognitive abnormalities (Ma *et al.* 2011). We theorized that structural connectivity in the DMN may exhibit abnormal organization in heroin abusers and be correlated with clinical characteristics of heroin addiction.

Heroin abusers exhibit impairments in multiple cognitive functions, especially high impulsivity and impulsive decision-making, which are critical risk factors for relapse (Bechara 2005). A growing body of evidence suggests that impulsivity and declines in decision-making in heroin abusers may arise from brain abnormalities, including dysfunctional structural and functional networks (Ersche *et al.* 2006; Xie *et al.* 2011; Qiu *et al.* 2013). Additionally, brain abnormalities in heroin abusers may be significantly associated with drug use characteristics (e.g. the duration and dosage of heroin use; Yuan *et al.* 2010; Seifert *et al.* in press). Therefore, we investigated whether brain structural network changes are related to impairments in neurocognitive performance, including global cognition, impulsivity, decision-making and drug use characteristics in heroin addiction.

MATERIAL AND METHODS

Participants

This study was a cross-sectional design that was performed in accordance with the Declaration of Helsinki and was approved by the Research Ethics Board at Peking University. Seventy-six heroin-dependent individuals were recruited from Zhongshan Compulsory Detoxification Institute, Guangdong Province, China. They met the *Diagnostic and Statistical Manual of Mental Disorders*, 4th edition, criteria for heroin dependence but did not have any other substance dependence history (other opioid drug use for not more than 1 month and other kinds of addictive drug use not more than three times), with the exception of nicotine dependence (according to medical records and self-reports). The subjects had been abstinent from heroin for 1 month to 1 year at the time of the study. The inclusion criteria were the following: Zhongshan origin, male, 30–50 years old, right-handed and intravenous heroin use. None of the heroin-dependent patients received systemic pharmacological substitution treatments during the study. Seventy-eight age-matched healthy male controls were enrolled using advertisements in the local newspaper. Control subjects were excluded if they had any history of drug abuse or dependence other than nicotine. No participants were currently taking antipsychotics, benzodiazepines, antiparkinson medications or anticholinergics. Other exclusion criteria were the following: history of head injury with loss of consciousness, current or past major Axis I psychiatric disorder (including their first-degree relatives), history of cardiovascular or endocrine diseases and imaging scan contraindications (such as claustrophobia, dentures, head trauma and metal implants). Alcohol abusers were excluded based on the Michigan Alcoholism Screening Test. All included subjects were determined by the structured clinical interview. The participants provided written informed consent after a detailed explanation of the procedures and risks of the study. The subjects received monetary compensation for participating in the study.

Neuropsychological test

The participants underwent a detailed battery of standardized neuropsychological tests either on the same

day or within a few days of their MRI scanning. We focused our analysis on the following four cognitive tests.

(i) Montreal cognitive assessment (MoCA): The MoCA is a cognitive-screening test that is used to assess global cognitive ability (Nasreddine *et al.* 2005). It includes tests of visual space and execution, naming, memory, attention, language, abstraction, delayed recall and orientation. The MoCA takes approximately 10–15 minutes to administer and is scored on a 30-point scale. A higher score indicates better cognitive function, and the cutoff score is 24/25.

(ii) Barratt impulsiveness scale (BIS-11): The BIS-11 is a well-validated self-report measure of impulsivity (Patton, Stanford, & Barratt 1995). The BIS is a 30-item self-report questionnaire that assesses impulsive personality traits in three dimensions: attention (inattention and cognitive instability), motor behavior (spontaneous actions) and non-planning (lack of forethought). Subjects were administered the Chinese version.

(iii) Iowa gambling task (IGT): The IGT is a common measure of decision-making (Bechara *et al.* 1994), which is a card-playing task-assessing decision-making under uncertainty and risk. In the IGT, a disadvantageous decision bias is reflected by a preference for card decks that are associated with high immediate wins but long-term losses. The IGT net score [sum of advantageous deck choices (C + D) minus sum of disadvantageous deck choices (A + B)] is an index of the quality of decision-making.

(iv) Visual analogue scale (VAS). A VAS was used to assess heroin craving at rest on a 10-point scale, from 'not at all' to 'extremely' (Bickel, DeGrandpre, & Higgins 1993).

Magnetic resonance imaging data acquisition

Magnetic resonance imaging was performed using a 1.5-T MR Signa HDxt imaging system (General Electric Medical System, Milwaukee, WI, USA) and standard eight-channel head coil. The routine MRI sequences included T2 fluid-attenuated inversion recovery. T1-weighted, sagittal three-dimensional images were acquired with a spoiled gradient recalled echo sequence with coverage of the entire brain (slice thickness, 1 mm; repetition time/echo time, 7.816 ms/2.984 ms; inversion time, 450 ms; flip angle, 13°; acquisition matrix, 256 × 256; field of view, 256 × 256 mm^2; number of averages, 2). For DTI, a total of 28 image sets were acquired with 56 axial slices (slice thickness, 2.4 mm with no gap, repetition time/echo time, 14.4 s/85 ms; three *b*0 images without diffusion weighting and 25 non-collinear diffusion-weighting gradients with a *b* value of 1000 s/mm^2; acquisition matrix, 128 × 128; field of view, 256 × 256 mm^2). Two experienced radiologists checked the T2 images, and no abnormal brain structures were found in the subjects.

Data preprocessing

The data preprocessing consisted of the following steps: eddy current and motion artifact correction of the DTI data (FSL version 4.1.9; http://www.fmrib.ox.ac.uk/fsl; accessed April 27, 2015), estimation of the diffusion tensor, calculation of the diffusion metrics and reconstruction of the whole brain white matter tracts. Distortions in the diffusion-weighted images that were caused by eddy currents and head motions were corrected by applying an affine alignment of each diffusion-weighted image to the $b = 0$ image. Gradient directions were adjusted to account for any slight rotations associated with head movement (Leemans & Jones 2009). Diffusion tensor models were estimated by solving the Stejskal and Tanner equation, and FA and other diffusion metrics were calculated at each voxel. Whole brain white matter fiber tracts were reconstructed in native diffusion space for each subject using the fiber assignment by continuous tracking algorithm (Mori *et al.* 1999), embedded in DTI studio (version 3.0.3). All of the tracts in the dataset were reconstructed by seeding voxels with an FA value that was greater than 0.2. Fiber tracking was initiated from the center of each seed voxel and stopped when the angle between two consecutive orientation vectors was greater than the given threshold of 45°or reached voxels where FA was less than 0.2.

Network construction

Nodes and edges are two basic elements of a network. In the present study, we defined all of the network nodes and edges using the following procedures (for a flow chart, see Fig. S1).

Network node definition

The procedure that was used to define the nodes has been described previously (Shu *et al.* 2011) and was performed using SPM8 software (http://www.fil.ion.ucl.ac.uk/spm/software/spm8; accessed April 27, 2015). Briefly, individual T1-weighted images were first co-registered to the *b*0 image in the native DTI space. The transformed T1 images were then non-linearly transformed into the ICBM152 T1 template in MNI space. The inverse transformations were used to warp the automated anatomical labeling atlas from the MNI space to the native DTI space with a nearest-neighbor interpolation method. Using this procedure, we obtained 90 cortical and subcortical regions (45 for each hemisphere), with each representing a node of the network.

Network edge definition

To define the network edges between the 90 regions, we selected a threshold value for the streamline bundles. Two regions were considered structurally connected if at least three streamlines with two endpoints were located in each pair of two regions. Such a threshold selection reduced the risk of false-positive connections because of noise or limitations in the deterministic tractography and simultaneously ensured the size of the largest connected subnetwork that was observed in the networks across all of the controls (Shu *et al.* 2011). After the network edges were defined, the weighted network analyses were performed. Specifically, we defined the streamline number (SN) of the connected streamlines between each pair of regions as the weights of the network edges. As a result, we constructed the SN-weighted white matter network for each participant, which was represented by a symmetrical 90×90 matrix.

Network analysis

To characterize the topological organization of white matter structural networks, several graph measures were considered: network strength, global efficiency, local efficiency, shortest path length, clustering coefficient and small-worldness. The uses and interpretations of these network measures (Rubinov & Sporns 2010) are the following.

Network strength

The strength of a network is the average of the strength across all of the nodes in the network. For a network (graph) G with N nodes and K edges, we calculated the strength of G as the following:

$$\mathrm{S_P(G)} = \frac{1}{\mathrm{N}} \sum_{i \in G} S(i)$$

where S(i) is the sum of the edge weights w_{ij} (w_{ij} are the SN values between node i and node j) linking to node i. The strength of a network is the average of the strength across all of the nodes in the network. To control for the effects of the different number of total streamlines on the network topological differences, the connectivity matrix of each subject was first normalized to the network strength (the total number of interconnecting streamlines between regions) before the calculation of the following network properties.

Small-world properties

Small-world network parameters (clustering coefficient, C_p, and shortest path length, L_p) were originally proposed by Watts and Strogatz (Watts & Strogatz 1998). In the present study, we investigated the small-world properties of the weighted brain networks (Rubinov & Sporns 2010). The clustering coefficient of a node i, C(i), which was defined as the likelihood of whether the neighborhoods were connected with each other or not, was computed as the following:

$$\mathrm{C(i)} = \frac{2}{k_i(k_i - 1)} \sum_{j,k} \left(\overline{w}_{ij}\overline{w}_{jk}\overline{w}_{ki}\right)^{1/3}$$

where k_i is the degree of node i and $\overline{w}$ is the weight, which is scaled by the mean of all weights to control the cost of each participant at the same level. The clustering coefficient is zero [C(i) = 0] if the nodes are isolated or have just one connection (i.e. $k_i = 0$ or $k_i = 1$). The clustering coefficient, C_p, of a network is the average of the clustering coefficient over all nodes and indicates the extent of local interconnectivity or cliquishness in a network.

The path length between any pair of nodes (e.g. node i and node j) is defined as the sum of the edge lengths along this path. For weighted networks, the length of each edge was assigned by computing the reciprocal of the edge weight, $1/w_{ij}$. The shortest path length, L_{ij}, is defined as the length of the path for node i and node j with the shortest length. The shortest path length of a network was computed as the following:

$$L_p = \frac{1}{N(N-1)} \sum_{i \neq j \in G} L_{ij}$$

where N is the number of nodes in the network. The L_p of a network quantifies the ability for information to propagate in parallel.

To examine small-world properties, the clustering coefficient, C_p, and the shortest path length, L_p, of the brain networks were compared with those of random networks. In the present study, we generated 100 matched random networks, which had the same number of nodes, edges and degree distribution as the real networks (Maslov & Sneppen 2002). Notably, we retained the weight of each edge during the randomization procedure such that the weight distribution of the network was preserved. Furthermore, we computed the normalized shortest path length λ ($\lambda = L_p^{\mathrm{real}}/Lp_p^{\mathrm{rand}}$) and normalized clustering coefficient γ ($\gamma = C_p^{\mathrm{real}}/C_p^{\mathrm{rand}}$), where L_p^{rand} and C_p^{rand} are the mean clustering coefficient and mean shortest path length of 100 matched random networks, respectively. Importantly, two parameters correct differences in the edge number and degree distribution of the networks across individuals. A real network would be considered small-world if $\gamma > 1$ and $\lambda \approx 1$ (Watts & Strogatz 1998). Thus, a small-world network not only has a higher local

interconnectivity but also has the shortest path length that is approximately equivalent to that of random networks. These two measurements can be summarized into a simple quantitative metric, small-worldness ($\sigma = \gamma/\lambda$), which is typically $\sigma > 1$ for small-world networks (Humphries, Gurney, & Prescott 2007).

Network efficiency

The global efficiency of G measures the global efficiency of parallel information transfer in the network (Latora & Marchiori 2001), which can be computed as the following:

$$E_{\text{glob}}(G) = \frac{1}{N(N-1)} \sum_{i \neq j \in G} \frac{1}{L_{ij}}$$

where L_{ij} is the shortest path length between node i and node j in G.

The local efficiency of G reveals how much the network is fault-tolerant and shows the efficiency of communication among the first neighbors of node i when it is removed. The local efficiency of a graph is defined as the following:

$$\mathrm{E}_{\text{loc}}(G) = \frac{1}{N} \sum_{i \in G} E_{\text{glob}}(G_i)$$

where G_i denotes the subgraph that is composed of the nearest neighbors of node i.

Network connectivity characteristics

To further localize specific pairs of brain regions where structural connections were altered in the patients, we used an NBS approach (Zalesky *et al.* 2010), which is a non-parametric multiple-comparison procedure that identifies differences in network connectivity. We identified regional pairs that showed between-group differences in structural connectivity and further localized connected networks that showed significant changes in heroin abusers (for details, see the Statistical analysis section in the following).

Tract-based spatial statistic analysis

To determine group-level differences in white matter integrity, we performed tract-based spatial statistic analysis (TBSS) using the FMRIB Software Library. The FA image of each subject was aligned to a pre-identified target FA image (FMRIB58_FA) by non-linear registration. All of the aligned FA images were transformed into the MNI152 template ($1 \times 1 \times 1$ mm) by affine registration. The mean FA image and its skeleton (i.e. the mean FA skeleton) were created from all of the subjects. Fractional anisotropy images from individual subjects were projected onto the skeleton. Voxel-wise statistics across subjects were calculated for each voxel on the common skeleton. Tract identification of the locations of white matter structures was based on the JHU White-Matter Tractography Atlas. The cerebellum was excluded from the image analysis. To better visualize the results, the data were thickened with the 'tbss-fill' command.

Voxel-wise statistics in TBSS were performed using a permutation-based inference tool for non-parametric statistical threshold. The mean FA skeleton was used as a mask (threshold at a mean FA value of 0.2), and the number of permutations was set to 5000. The FA values were first corrected by false discovery rate correction ($P < 0.05$). If no results were significant after false discovery rate correction, then we tried to use AlphaSim correction. The statistical threshold of AlphaSim correction was set at porigin <0.01 and cluster size >5 voxels, corresponding to a corrected $P < 0.05$. This correction was confined within the group FA skeleton mask (thresholded at 0.2) and was determined using Monte Carlo simulations and the AFNI AlphaSim program (http://afni.nih.gov/afni/docpdf/AlphaSim.pdf; accessed April 27, 2015).

Statistical analysis

The two-sample t-test was used to test differences in demographic characteristics between groups using SPSS 16.0 software. To determine differences in neurocognitive performance and global network metrics between groups (S_p, C_p, L_p, E_{glob}, E_{loc}, γ, λ and σ), a multiple linear regression analysis was performed, with age and cigarettes smoked per day as covariates.

The NBS approach was utilized to identify network connectivity differences between heroin abusers and healthy controls and conducted within the connections. Briefly, a primary threshold ($P < 0.05$) was first applied to the one-tailed test of the general linear model that was computed for each link to define a set of suprathreshold links, among which any connected subnetworks and their sizes (number of links) were then determined, obtaining increases or decreases in subnetworks in the patients separately. To estimate the significance for each subnetwork, the null distribution of the connected subnetwork size was empirically derived using a non-parametric permutation approach (10 000 permutations). For each permutation, all of the subjects were randomly re-allocated to two groups, and the general linear model was computed independently for each link. The threshold ($P < 0.05$) was then used to generate suprathreshold links among which the maximal connected subnetwork size was recorded. Finally, for a connected subnetwork size (M) that was found in a right grouping of controls and patients, the corrected P value was determined by finding the proportion of the 10 000 permutations for which the maximal connected

subnetwork was larger than M. Age and cigarettes smoked per day were used as covariates in the regression analysis of each connection.

When significant between-group differences were observed in any network metrics and network connectivity, we further assessed the relationships between these metrics and network connectivity with the clinical and psychological characteristics in the heroin addiction group, which was performed by partial correlation analyses with cigarettes smoked per day and age as covariates.

The network analysis was performed using the GRETNA package (http://www.nitrc.org/projects/gretna/; accessed April 27, 2015). The results were visualized using the BrainNet Viewer package (http://www.nitrc.org/projects/bnv/; accessed April 27, 2015).

RESULTS

Demographics and neurocognitive performance

No significant difference was found in the demographic characteristics of the subjects, with the exception of the number of cigarettes smoked per day, which was significantly higher in heroin abusers than in controls. Compared with healthy controls, heroin abusers had significantly lower MoCA and IGT scores and higher motor and non-planning scores on the BIS-11 (Table 1).

Table 1 Demographic and heroin use characteristics and neurocognitive performance of the subjects.

	Heroin group (n = 76)	*Control group (n = 78)*	*P*
Age (years)	36.22 ± 3.93	37.58 ± 4.99	*0.064*
Gender (male/female)	76/0	78/0	N.A.
Cigarettes smoked per day	26.16 ± 9.16	8.83 ± 9.82	<0.001
Heroin dosage (g/day)	0.52 ± 0.36	N.A.	N.A.
Abstinence time (months)	5.48 ± 3.44	N.A.	N.A.
Heroin duration of use (years)	15.13 ± 3.45	N.A.	N.A.
Heroin craving at rest	2.93 ± 0.24	N.A.	N.A.
MoCA score	26.64 ± 0.38	22.01 ± 0.29	<0.001
IGT score	3.59 ± 3.23	−4.64 ± 2.44	0.039
BIS-11 score (attention)	15.72 ± 0.39	16.89 ± 0.31	0.011
BIS-11 score (motivation)	20.72 ± 0.58	23.87 ± 0.52	0.0084
BIS-11 score (non-planning)	24 ± 0.84	27.42 ± 0.62	0.020
BIS-11 score (sum)	60.44 ± 1.49	68.18 ± 1.05	0.0012

BIS = Barratt Impulsiveness Scale; IGT = Iowa Gambling Task; MoCA = Montreal Cognitive Assessment; N.A. = not applicable. The data are expressed as mean ± standard error.

Whole brain mapping of connectivity deficits in heroin abusers

The NBS identified one extensive subnetwork that was increased (34 nodes and 35 edges) and significantly different between heroin abusers and control participants ($P = 0.0021$ after the 10 000 permutation test; Fig. 1a). This subnetwork could be generally categorized into three systems: default-mode, attentional and visual. The default-mode system mainly involved the bilateral medial superior frontal gyrus, superior temporal pole, left inferior parietal gyrus, bilateral precuneus and cingulate regions. The attentional system mainly consisted of the bilateral superior frontal gyrus, supplementary motor area and superior parietal gyrus. The visual system mainly included the bilateral superior occipital gyrus, lingual gyrus and right fusiform. The details of the increased connections and nodes within the subnetwork are illustrated in Tables 2 and S1.

Individuals with heroin dependence had widespread increases in FA compared with healthy controls (Fig. 1b). The increase in FA was mainly located in the corpus callosum, inferior longitudinal fasciculus, superior longitudinal fasciculus and forceps major. The main clusters are listed in Table S2.

Correlation analyses revealed that the mean FA value within the increased clusters in the TBSS analysis was positively correlated with the streamline number within the increased subnetwork in the NBS analysis (Fig. 1c)

Global network properties

We found no significant differences in any global parameter (average strength, global and local efficiency, L_p, C_p, λ, γ and σ) of the whole brain anatomical networks between the two groups (Table 3). Both heroin abusers and the healthy controls exhibited efficient small-world properties in the white matter networks, characterized by almost identical path lengths ($\lambda \approx 1$) but higher clustering coefficients ($\gamma > 1$) in the brain networks compared with the matched random networks (heroin abusers: $\gamma = 2.8449 \pm 0.0194$, $\lambda = 1.1697 \pm 0.0325$; healthy controls: $\gamma = 2.868 \pm 0.1636$, $\lambda = 1.1649 \pm 0.0307$).

Relationships between network metrics and clinical variables and performance

No significant correlation was found between any global network parameters, including average strength, global

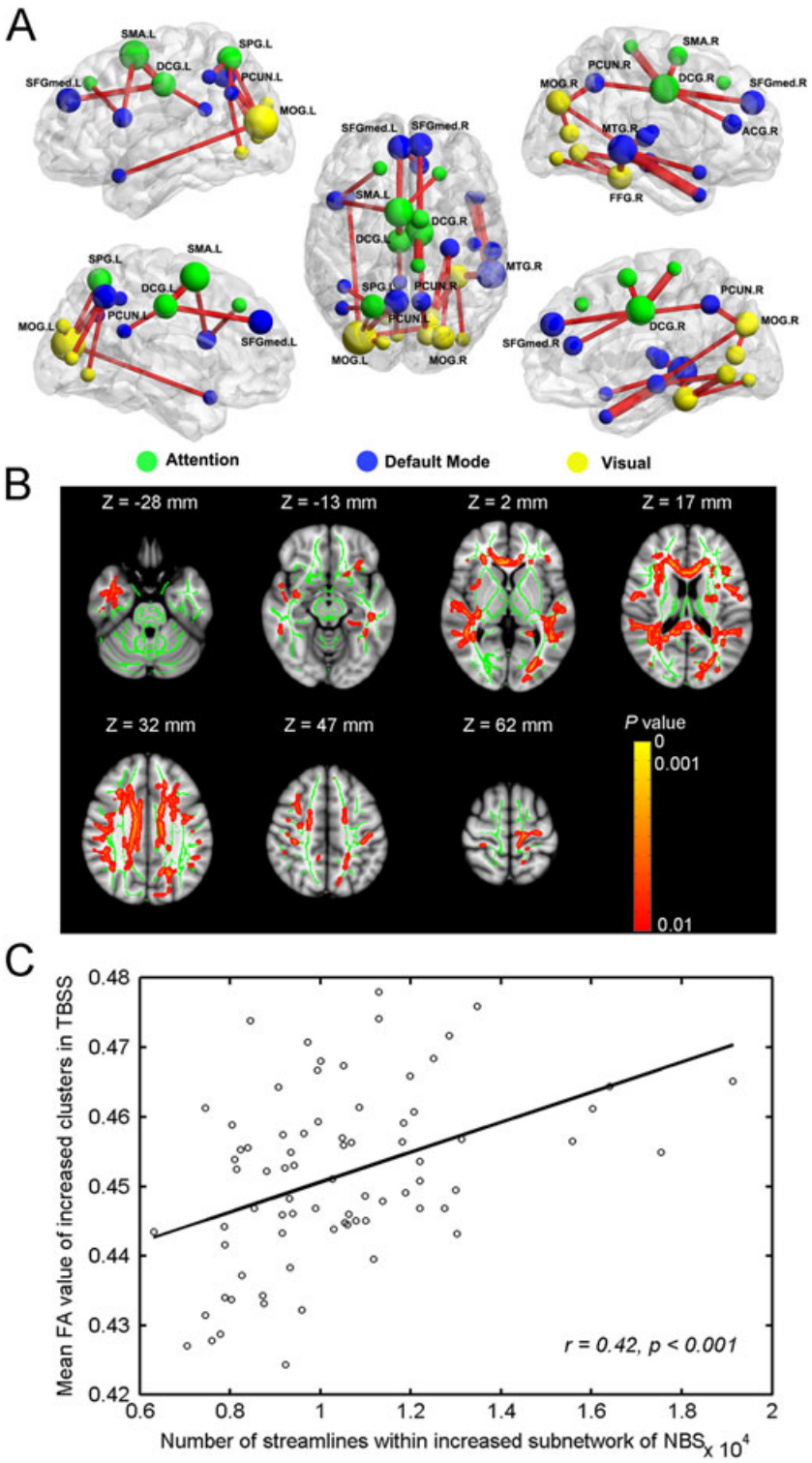

Figure 1 Network-based statistic (NBS) and tract-based spatial statistical (TBSS) analysis results. (a) Heroin abusers relative to the control subjects showed increased connectivity in a subnetwork composed of 34 nodes and 35 edges ($P = 0.0021$ after 10 000 permutation test). The subnetwork could be categorized into three systems: (1) the nodes in blue are within the default-mode system, mainly involving the bilateral medial superior frontal gyrus, the superior temporal pole, the left inferior parietal gyrus, the bilateral precuneus and cingulate regions; (2) the nodes in green are within the attentional system, including the bilateral superior frontal gyrus, supplementary motor area and superior parietal gyrus; and (3) the nodes in yellow are within the visual system, including the bilateral superior occipital gyrus, lingual gyrus and right fusiform. The node sizes indicate their connection number in this subnetwork. The edge width represents the *T* value between groups. For details on the increased connections and nodes within the subnetwork, see Tables 2 and S1. (b) Regions that showed significant increases in fractional anisotropy (FA) in heroin abusers compared with healthy controls (AlphaSim-corrected $P < 0.05$). The FA values were higher mainly in the corpus callosum, inferior longitudinal fasciculus, superior longitudinal fasciculus and forceps major. Details on the main clusters with increases in FA in heroin abusers are depicted in Table S2. (c) Mean FA values within the increased clusters in the TBSS analysis were positively correlated with the streamline number within the increased subnetwork in the NBS analysis

and local efficiency, L_p, C_p, λ, γ and σ, and clinical performance (global cognition, decision-making and impulsivity; all $P > 0.05$).

We found a significant positive correlation between the connection strength of the left superior frontal gyrus and the left opercular inferior frontal gyrus (SFG.L-SFGoperc.L) with the daily dosage of heroin ($P = 0.0022$). A negative correlation was found between the connection strength of the right middle temporal gyrus and right middle temporal pole (MTG.R-TPOmid.R) and non-planning scores on the BIS-11 ($P = 0.0087$; Fig. 2).

Table 2 White matter connections of increase in network-based statistic subnetwork in heroin abusers.

Connection	*Connection strength (mean ± standard deviation)*		
	Heroin group (n = 76)	*Control group (n = 78)*	*t*
Left opercular inferior frontal and left superior frontal	80.00 ± 87.44	55.29 ± 76.67	3.84
Left supplementary motor area and right superior frontal	50.93 ± 76.48	35.72 ± 53.28	2.99
Left opercular inferior frontal and left supplementary motor area	91.25 ± 94.64	54.67 ± 93.29	2.78
Left supplementary motor area and right supplementary motor area	227.99 ± 261.74	190.82 ± 190.31	2.71
Right medial superior frontal and left medial superior frontal	568.75 ± 405.51	509.51 ± 373.04	2.67
Left medial superior frontal and right anterior cingulate	87.59 ± 81.84	77.40 ± 75.04	2.58
Left supplementary motor area and left middle cingulate	119.49 ± 61.69	109.36 ± 56.61	2.52
Left medial superior frontal and left middle cingulate	143.30 ± 117.40	113.12 ± 79.43	2.4
Right supplementary motor area and right middle cingulate	115.26 ± 69.60	117.49 ± 53.87	2.36
Right medial superior frontal and right middle cingulate	90.83 ± 69.1	81.01 ± 54.4	2.35
Right anterior cingulate and right middle cingulate	225.5 ± 94.20	189.51 ± 93.94	2.35
Left posterior cingulate and left middle cingulate	39.54 ± 33.8	30.54 ± 23.52	2.33
Right hippocampus and right lingual	103.26 ± 84.36	82.24 ± 70.19	2.27
Right hippocampus and right superior occipital	39.08 ± 38.42	31.32 ± 35.65	2.24
Right superior occipital and right calcarine	86.24 ± 48.18	74.82 ± 37.68	2.23
Right superior occipital and right cuneus	208.82 ± 78.09	207.91 ± 76.89	2.16
Left middle occipital and right calcarine	102.78 ± 109.09	58.44 ± 59.53	2.13
Left middle occipital and left superior occipital	352.12 ± 128.83	335 ± 119.71	2.12
Right lingual and right fusiform	194.22 ± 77.89	186.42 ± 69.81	2.11
Right inferior occipital and right fusiform	301.41 ± 148.15	274.51 ± 116.53	2.09
Left superior parietal and left middle occipital	262.84 ± 135.28	228.37 ± 110.94	2.04
Left inferior parietal and left superior parietal	291.08 ± 131.04	266.59 ± 139.16	1.99
Left angular and left superior parietal	82.46 ± 70.89	72.44 ± 95.95	1.97
Left precuneus and left calcarine	133.03 ± 60.42	118.40 ± 49.33	1.95
Left precuneus and left lingual	69.25 ± 34.57	61.62 ± 34.38	1.94
Left precuneus and left medial occipital	28.50 ± 58.26	24.38 ± 41.07	1.93
Right precuneus and right medial superior frontal	206.39 ± 107.30	109.58 ± 94.72	1.91
Right precuneus and right cuneus	30.45 ± 43.24	23.33 ± 31.08	1.91
Right paracentral lobule and right middle cingulate	29.75 ± 23.49	24.03 ± 17.74	1.83
Right superior temporal and right Heschl	45.72 ± 30.48	33.81 ± 20.39	1.79
Left superior temporal pole and left middle occipital	24.84 ± 27.29	21.94 ± 30.09	1.76
Right middle temporal and right fusiform	33.87 ± 56.09	18.23 ± 25.35	1.75
Right middle temporal and right superior temporal	564.24 ± 184.82	489.90 ± 173.90	1.7
Right superior temporal pole and right middle temporal	50.96 ± 36.97	48 ± 26.42	1.67
Right middle temporal pole and right middle temporal	104.37 ± 60.04	80.73 ± 41.69	1.66

Table 3 Global network metrics in heroin abusers and controls.

Global network parameter	*Heroin group (n = 76)*	*Control group (n = 78)*	*t*	*P*
Average strength	1107.76 ± 157.49	1113.43 ± 154.04	1.58	0.12
Global efficiency	0.79 ± 0.046	0.79 ± 0.046	−0.17	0.86
Local efficiency	1.12 ± 0.053	1.13 ± 0.050	−0.65	0.52
L_p	1.27 ± 0.076	1.26 ± 0.073	0.20	0.84
C_p	0.57 ± 0.015	0.58 ± 0.016	−0.86	0.39
λ	1.17 ± 0.033	1.16 ± 0.030	1.43	0.15
γ	2.84 ± 0.019	2.87 ± 0.16	−0.96	0.34
σ	2.43 ± 0.17	2.46 ± 0.15	−1.53	0.13

Values are expressed as mean ± standard deviation.

DISCUSSION

The present study explored differences in whole brain structural networks between heroin abusers and healthy controls in a large sample. One increased subnetwork characterizing widespread abnormalities in structural connectivity was present in heroin users, including the default-mode, attentional and visual systems. The connection strength was positively correlated with increases in FA in heroin abusers. Furthermore, the connection strength of SFG.L-IFGoperc.L increased as the daily dosage of heroin increased. The non-planning impulsivity trait was negatively associated with an increase in the connection strength of MTG.R-TPOmid.R in heroin abusers. Our results indicated that structural connectivity was extensively reorganized in heroin

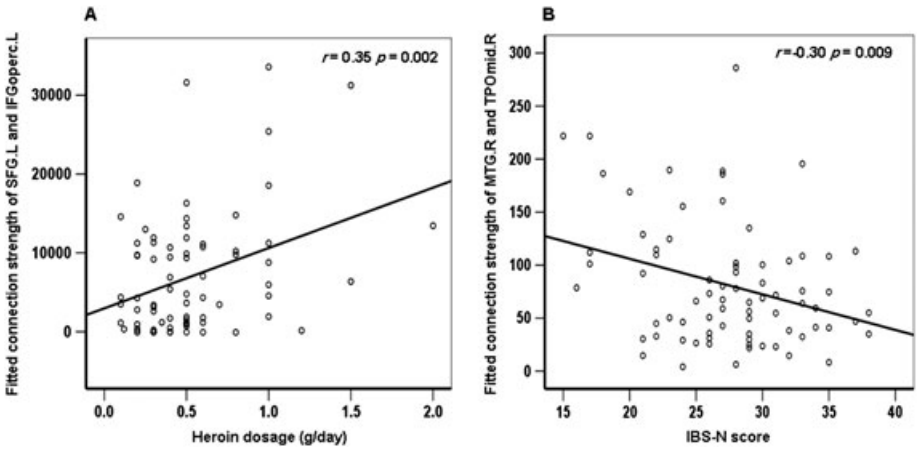

Figure 2 Relationships between network metrics and clinical variables and performance in heroin-dependent individuals. (a) A significant positive correlation was found between the connection strength of the pathway that connects the left superior frontal gyrus (SFG.L) and left opercular inferior frontal gyrus (IFGoperc.L) and daily dosage of heroin use ($P = 0.0022$). (b) A negative correlation was found between the connection strength of the pathway that connects the right middle temporal gyrus (MTG.R) and right middle temporal pole (TPOmid.R) and non-planning scores (N) on the BIS-11 ($P = 0.0087$)

abusers, and the connectivity properties were correlated with heroin addiction-related clinical variables and performance.

As expected, the DMN that was previously identified as dysfunctional in heroin abusers showed abnormal structural connectivity. The precuneus is a functional core of the DMN (Utevsky, Smith, & Huettel 2014), and its activation may be involved in cue reactivity in addiction disorders (Brody *et al.* 2007). Areas in the frontal part of the DMN are implicated in both the excitatory and inhibitory modulation of craving associated with addiction (Sell *et al.* 2000; Rose *et al.* 2011). The hippocampus is a prominent node within the DMN and the main brain region involved in learning drug-related cues that drive relapse to drug-seeking behavior (Robbins, Ersche, & Everitt 2008). Thus, the increase in the connectivity of the DMN in heroin abusers may suggest hypersensitivity to drug-related cues and enhanced addiction-related memory processing. The attentional network, which has opposite activational effects to the DMN through modulatory interactions (Hellyer *et al.* 2014), is implicated in attentional bias toward drug cues in substance-dependent individuals and contributes to the perpetuation of drug use (Hester & Luijten 2014). Previous studies found gray matter abnormalities in attentional network areas in heroin abusers, including superior parietal regions (Li *et al.* 2014) and the supplementary motor cortex (Liu *et al.* 2009). Thus, the co-disorganization of the DMN and attentional network could arise from an imbalance in continuous oscillation in these two systems (Kim 2014).

Consistent with the heroin-related changes in the pattern of resting-state functional connectivity (Ma *et al.* 2010; Yuan *et al.* 2010), the microstructural measures of white matter connectivity also increased in heroin abusers. We explored whether our findings of increases in white matter connectivity were driven by increases in FA. The TBSS analysis did reveal widespread increases in FA in heroin abusers, which was consistent with the changing pattern of white matter connectivity in heroin abusers (Fig. 1b). Furthermore, the increases in FA were positively correlated with the streamline number within the subnetwork that was increased (Fig. 1c). Thus, the increases in white matter connectivity may be attributable to more inefficient white matter microstructure integrity. With the deepening understanding of the imaging phenotype in psychosis disorders, the increased pattern in parameters of white matter is not always better, for which may predict anomalous cognitive function in some diseases (Hoeft *et al.* 2007). The FA is a well-established biomarker of white matter integrity, which may be affected by many factors, including myelination and axon size (Le Bihan 2003). The network strength, SN, may depend on the number and myelination of axons. The myelin sheath, which is wrapped by oligodendrocytes that can express opioid receptors, supports axon survival and function. Blocking opioid receptor activity decreases oligodendrogenesis (Persson *et al.* 2003). Therefore, heroin may increase white matter integrity by increasing the number of oligodendrocytes. However, our network findings are not completely consistent with alterations in the resting-state connectivity network that were previously reported in heroin users (Ma *et al.* 2011; Jiang *et al.* 2013). This may be because resting-state functional networks are variable and continually reconfigure around the underlying anatomical skeleton (Honey *et al.* 2009).

Modulations within and between brain networks are dynamic (Bassett *et al.* 2011). Based on the correlation analysis results, we may acquire an initial understanding of the cause of the increases in structural connectivity in heroin addiction. Our results showed that the changes in structural connections within frontal regions of the DMN were positively correlated with heroin dosage, suggesting that this connectivity abnormality was related to the severity of addiction. Additionally, a significant association was found between connectivity within the MTG and non-planning impulsivity in heroin abusers. This finding is consistent with a recent study that found that the MTG is significantly hypoactive during No-Go trials (Ding *et al.* 2014), suggesting that the MTG plays an inhibitory role in impulsivity traits.

Some issues should be addressed. First, we performed a cross-sectional study, and our results did not clearly indicate whether the changes in network features were a cause or consequence of heroin addiction. Second, structural connectivity may be mirrored by functional networks, but this may not be presumed to be a one-to-one correspondence (Wang *et al.* 2015). Therefore, combining information on structural and functional connectivity may clarify how structural disruption underlies functional deficits in heroin users. Third, the changes in structural networks should be generalized in female participants and by high-field MRI.

In conclusion, we found that heroin abuse was associated with increases in structural connectivity within the DMN and attentional and visual systems. Specific within-frontal and within-temporal connections were significantly correlated with clinical measures in heroin abusers. Our findings revealed a structural basis for alterations in functional connectivity and neurocognitive impairments in heroin abusers and suggested that disruptions in connectivity in heroin addiction may be attributable to inefficient white matter microstructure integrity.

Acknowledgements

This work was supported by the National Basic Research Program of China (no. 2015CB553503), National Science Fund for Distinguished Young Scholars (no. 81225009) and National Natural Science Foundation of China (no. U1402226, 81221002 and 91132719). We thank the infirmary personnel at Zhongshan Addiction Treatment Center and the doctors at Zhongshan Traditional Chinese Medicine Hospital for help with data acquisition and Prof. Rui-Wang Huang for technical support. All of the authors had full access to all of the data in the study and take responsibility for the integrity of the data and accuracy of the data analysis.

Authors Contribution

JS and YH chose the topic, defined the scope of the study and obtained funding for the study. YS and G-BW designed the research, developed the protocol, performed the research and wrote the first draft of the manuscript. Q-XL analyzed the data and assisted with writing the manuscript. NS and JW provided guidance and assisted with the data analyses. LL, H-BH and S-QM assisted with writing the manuscript and provided critical revisions for important intellectual content. All of the authors critically reviewed the content and approved the final version for publication.

References

Bassett DS, Wymbs NF, Porter MA, Mucha PJ, Carlson JM, Grafton ST (2011) Dynamic reconfiguration of human brain networks during learning. Proc Natl Acad Sci U S A 108:7641–7646.

Bechara A (2005) Decision making, impulse control and loss of willpower to resist drugs: a neurocognitive perspective. Nat Neurosci 8:1458–1463.

Bechara A, Damasio AR, Damasio H, Anderson SW (1994) Insensitivity to future consequences following damage to human prefrontal cortex. Cognition 50:7–15.

Behrens TE, Sporns O (2012) Human connectomics. Curr Opin Neurobiol 22:144–153.

Bickel WK, DeGrandpre RJ, Higgins ST (1993) Behavioral economics: a novel experimental approach to the study of drug dependence. Drug Alcohol Depend 33:173–192.

Bora E, Yucel M, Fornito A, Pantelis C, Harrison BJ, Cocchi L, Pell G, Lubman DI (2012) White matter microstructure in opiate addiction. Addict Biol 17:141–148.

Brody AL, Mandelkern MA, Olmstead RE, Jou J, Tiongson E, Allen V, Scheibal D, London ED, Monterosso JR, Tiffany ST, Korb A, Gan JJ, Cohen MS (2007) Neural substrates of resisting craving during cigarette cue exposure. Biol Psychiatry 62:642–651.

Buckner RL, Andrews-Hanna JR, Schacter DL (2008) The brain's default network: anatomy, function, and relevance to disease. Ann N Y Acad Sci 1124:1–38.

Bullmore E, Sporns O (2009) Complex brain networks: graph theoretical analysis of structural and functional systems. Nat Rev Neurosci 10:186–198.

Ding WN, Sun JH, Sun YW, Chen X, Zhou Y, Zhuang ZG, Li L, Zhang Y, Xu JR, Du YS (2014) Trait impulsivity and impaired prefrontal impulse inhibition function in adolescents with internet gaming addiction revealed by a Go/No-Go fMRI study. Behav Brain Funct 10:20.

Ersche KD, Fletcher PC, Roiser JP, Fryer TD, London M, Robbins TW, Sahakian BJ (2006) Differences in orbitofrontal activation during decision-making between methadone-maintained opiate users, heroin users and healthy volunteers. Psychopharmacology (Berl) 188:364–373.

Hagmann P, Cammoun L, Gigandet X, Meuli R, Honey CJ, Wedeen VJ, Sporns O (2008) Mapping the structural core of human cerebral cortex. PLoS Biol 6:e159.

Hellyer PJ, Shanahan M, Scott G, Wise RJ, Sharp DJ, Leech R (2014) The control of global brain dynamics: opposing actions

of frontoparietal control and default mode networks on attention. J Neurosci 34:451–461.

Hester R, Luijten M (2014) Neural correlates of attentional bias in addiction. CNS Spectr 19:231–238.

Hoeft F, Barnea-Goraly N, Haas BW, Golarai G, Ng D, Mills D, Korenberg J, Bellugi U, Galaburda A, Reiss AL (2007) More is not always better: increased fractional anisotropy of superior longitudinal fasciculus associated with poor visuospatial abilities in Williams syndrome. J Neurosci 27:11960–11965.

Honey CJ, Sporns O, Cammoun L, Gigandet X, Thiran JP, Meuli R, Hagmann P (2009) Predicting human resting-state functional connectivity from structural connectivity. Proc Natl Acad Sci U S A 106:2035–2040.

Hu W, Fu X, Qian R, Wei X, Ji X, Niu C (2012) Changes in the default mode network in the prefrontal lobe, posterior cingulated cortex and hippocampus of heroin users. Neural Regen Res 7:1386–1391.

Hulse GK, English DR, Milne E, Holman CD (1999) The quantification of mortality resulting from the regular use of illicit opiates. Addiction 94:221–229.

Humphries MD, Gurney K, Prescott TJ (2007) Is there a brainstem substrate for action selection? Philos Trans R Soc Lond B Biol Sci 362:1627–1639.

Jiang G, Wen X, Qiu Y, Zhang R, Wang J, Li M, Ma X, Tian J, Huang R (2013) Disrupted topological organization in whole-brain functional networks of heroin-dependent individuals: a resting-state FMRI study. PLoS One 8: e82715.

Kim H (2014) Encoding and retrieval along the long axis of the hippocampus and their relationships with dorsal attention and default mode networks: the HERNET model. Hippocampus 25:500–510.

Latora V, Marchiori M (2001) Efficient behavior of small-world networks. Phys Rev Lett 87:198701.

Le Bihan D (2003) Looking into the functional architecture of the brain with diffusion MRI. Nat Rev Neurosci 4:469–480.

Leemans A, Jones DK (2009) The B-matrix must be rotated when correcting for subject motion in DTI data. Magn Reson Med 61:1336–1349.

Li M, Tian J, Zhang R, Qiu Y, Wen X, Ma X, Wang J, Xu Y, Jiang G, Huang R (2014) Abnormal cortical thickness in heroin-dependent individuals. Neuroimage 88:295–307.

Liu H, Hao Y, Kaneko Y, Ouyang X, Zhang Y, Xu L, Xue Z, Liu Z (2009) Frontal and cingulate gray matter volume reduction in heroin dependence: optimized voxel-based morphometry. Psychiatry Clin Neurosci 63:563–568.

Liu H, Li L, Hao Y, Cao D, Xu L, Rohrbaugh R, Xue Z, Hao W, Shan B, Liu Z (2008) Disrupted white matter integrity in heroin dependence: a controlled study utilizing diffusion tensor imaging. Am J Drug Alcohol Abuse 34: 562–575.

Ma N, Liu Y, Fu XM, Li N, Wang CX, Zhang H, Qian RB, Xu HS, Hu X, Zhang DR (2011) Abnormal brain default-mode network functional connectivity in drug addicts. PLoS One 6: e16560.

Ma N, Liu Y, Li N, Wang CX, Zhang H, Jiang XF, Xu HS, Fu XM, Hu X, Zhang DR (2010) Addiction related alteration in resting-state brain connectivity. Neuroimage 49:738–744.

Maslov S, Sneppen K (2002) Specificity and stability in topology of protein networks. Science 296:910–913.

Mori S, Crain BJ, Chacko VP, van Zijl PC (1999) Three-dimensional tracking of axonal projections in the brain by magnetic resonance imaging. Ann Neurol 45:265–269.

Nasreddine ZS, Phillips NA, Bedirian V, Charbonneau S, Whitehead V, Collin I, Cummings JL, Chertkow H (2005) The Montreal Cognitive Assessment, MoCA: a brief screening tool for mild cognitive impairment. J Am Geriatr Soc 53:695–699.

Patton JH, Stanford MS, Barratt ES (1995) Factor structure of the Barratt Impulsiveness Scale. J Clin Psychol 51:768–774.

Persson AI, Thorlin T, Bull C, Zarnegar P, Ekman R, Terenius L, Eriksson PS (2003) Mu- and delta-opioid receptor antagonists decrease proliferation and increase neurogenesis in cultures of rat adult hippocampal progenitors. Eur J Neurosci 17:1159–1172.

Qiu Y, Jiang G, Su H, Lv X, Zhang X, Tian J, Zhuo F (2013) Progressive white matter microstructure damage in male chronic heroin dependent individuals: a DTI and TBSS study. PLoS One 8:e63212.

Robbins TW, Ersche KD, Everitt BJ (2008) Drug addiction and the memory systems of the brain. Ann N Y Acad Sci 1141:1–21.

Rose JE, McClernon FJ, Froeliger B, Behm FM, Preud'Homme X, Krystal AD (2011) Repetitive transcranial magnetic stimulation of the superior frontal gyrus modulates craving for cigarettes. Biol Psychiatry 70:794–799.

Rubinov M, Sporns O (2010) Complex network measures of brain connectivity: uses and interpretations. Neuroimage 52:1059–1069.

Seifert CL, Magon S, Sprenger T, Lang UE, Huber CG, Denier N, Vogel M, Schmidt A, Radue EW, Borgwardt S, Walter M (in press) Reduced volume of the nucleus accumbens in heroin addiction. Eur Arch Psychiatry Clin Neurosci.

Sell LA, Morris JS, Bearn J, Frackowiak RS, Friston KJ, Dolan RJ (2000) Neural responses associated with cue evoked emotional states and heroin in opiate addicts. Drug Alcohol Depend 60:207–216.

Shen Y, Wang E, Wang X, Lou M (2012) Disrupted integrity of white matter in heroin-addicted subjects at different abstinent time. J Addict Med 6:172–176.

Shu N, Liu Y, Li K, Duan Y, Wang J, Yu C, Dong H, Ye J, He Y (2011) Diffusion tensor tractography reveals disrupted topological efficiency in white matter structural networks in multiple sclerosis. Cereb Cortex 21:2565–2577.

Utevsky AV, Smith DV, Huettel SA (2014) Precuneus is a functional core of the default-mode network. J Neurosci 34:932–940.

Wang W, Wang YR, Qin W, Yuan K, Tian J, Li Q, Yang LY, Lu L, Guo YM (2010) Changes in functional connectivity of ventral anterior cingulate cortex in heroin abusers. Chin Med J (Engl) 123:1582–1588.

Wang Z, Dai Z, Gong G, Zhou C, He Y (2015) Understanding structural–functional relationships in the human brain: a large-scale network perspective. Neuroscientist 21:290–305.

Watts DJ, Strogatz SH (1998) Collective dynamics of 'small-world' networks. Nature 393:440–442.

Whitfield-Gabrieli S, Ford JM (2012) Default mode network activity and connectivity in psychopathology. Annu Rev Clin Psychol 8:49–76.

Xie C, Li SJ, Shao Y, Fu L, Goveas J, Ye E, Li W, Cohen AD, Chen G, Zhang Z, Yang Z (2011) Identification of hyperactive intrinsic amygdala network connectivity associated with

impulsivity in abstinent heroin addicts. Behav Brain Res 216:639–646.

Yuan K, Qin W, Liu J, Guo Q, Dong M, Sun J, Zhang Y, Liu P, Wang W, Wang Y, Li Q, Yang W, von Deneen KM, Gold MS, Liu Y, Tian J (2010) Altered small-world brain functional networks and duration of heroin use in male abstinent heroin-dependent individuals. Neurosci Lett 477:37–42.

Zalesky A, Fornito A, Bullmore ET (2010) Network-based statistic: identifying differences in brain networks. Neuroimage 53:1197–1207.

SUPPORTING INFORMATION

Additional Supporting Information may be found in the online version of this article at the publisher's web-site:

Table S1 The detailed nodal information of increased network-based statistic subnetwork in heroin abusers

Table S2 Main clusters (cluster size >100) of increased fractional anisotropy in heroin abusers

Figure S1 The flow chart of network analysis